Silver Supported on Titania as an Active Catalyst for Electrochemical Carbon Dioxide Reduction

Sichao Ma,[a, c] Yangchun Lan,[b, d] Gaby M. J. Perez,[b] Saman Moniri,[b] and
Paul J. A. Kenis *[b, c]

Although significant research efforts have focused on the exploration of catalysts for the electrochemical reduction of CO_2, considerably fewer reports have described how support materials for these catalysts affect their performance, which includes their ability to reduce the overpotential, and/or to increase the catalyst utilization and selectivity. Here Ag nanoparticles supported on carbon black (Ag/C) and on titanium dioxide (Ag/TiO_2) were synthesized. In a flow reactor, 40 wt% Ag/TiO_2 exhibited a twofold higher current density for CO production than 40 wt% Ag/C. Faradaic efficiencies of the 40 wt% Ag/TiO_2 catalyst exceeded 90% with a partial current density for CO of 101 mA cm^{-2}; similar to the performance of unsupported Ag nanoparticle catalysts (AgNP) but at a 2.5 times lower Ag loading. A mass activity as high as 2700 mA mg$_{Ag}^{-1}$ cm^{-2} was achieved. In cyclic voltammetry tests in a three-electrode cell, Ag/TiO_2 exhibited a lower overpotential for CO_2 reduction than AgNP, which, together with other data, suggests that TiO_2 stabilizes the intermediate and serves as redox electron carrier to assist CO_2 reduction while Ag assists in the formation of the final product, CO.

Introduction

The world's increasing energy consumption as a result of increases in the world population and increased energy consumption in developing parts of the world is accelerating the depletion of the world's dwindling fossil-fuel reserves.[1] This increased energy consumption has led to a steady increase in atmospheric CO_2 levels over several decades, which in turn has been linked to undesirable climate change effects. To curb the rise, and eventually to lower the atmospheric CO_2 levels, multiple approaches need to be pursued because no single approach has the capacity to address this issue by itself.[2] Approaches to reduce CO_2 emissions include switching to energy sources that emit less CO_2 (e.g., natural gas instead of coal), carbon capture and sequestration from point sources such as power plants, enhancing the energy efficiency of buildings and

cars, and the utilization of renewable sources such as solar and wind. Potential economic gains provide a natural incentive for the implementation of some of these approaches (e.g., enhancing the energy efficiency of buildings and cars), whereas other approaches will require regulation as they can only be implemented at a substantial cost (e.g., carbon capture and underground sequestration). Many renewable power plants (wind, solar, tidal, etc.) have become operational around the world but, because of their intermittent nature, these sources can only be used in combination with more conventional, fossil-fuel-based power plants. Furthermore, to avoid the waste of renewable power if the amount produced is high, methods for large-scale energy storage or on-demand utilization need to be developed.[3]

The catalytic conversion of CO_2 into useful chemicals such as intermediates for the synthesis of fuels and polymers by using photochemical, electrochemical, thermochemical, or other methods is another promising approach to curb atmospheric CO_2 levels, which provides the potential for economic gains at the same time.[4] More specifically, the electrochemical conversion of CO_2 into value-added products, such as formic acid, CO, hydrocarbons, or alcohols, can utilize on demand excess energy from renewable energy plants and help to reduce atmospheric CO_2 levels simultaneously.[5] However, significant improvements in the efficiency and at times the selectivity of the electrolysis of CO_2 into any of these products are needed for this process to become economically viable.[5, 6] Most electrocatalysts reported to date exhibit a high overpotential for the desired reaction, which drastically reduces the energy efficiency. Also, the conversion rate, as expressed by the observed current density, is still insufficient. Electrocatalysts need to be developed that simultaneously exhibit a low overpotential (thus

[a] S. Ma
Department of Chemistry
University of Illinois at Urbana-Champaign
505 South Mathews Avenue, Urbana, IL 61801 (USA)

[b] Y. Lan, G. M. J. Perez, S. Moniri, Prof. P. J. A. Kenis
Department of Chemical & Biomolecular Engineering
University of Illinois at Urbana-Champaign
600 South Mathews Avenue, Urbana, IL 61801 (USA)
Fax: (+1) 217-333-5052
E-mail: kenis@illinois.edu

[c] S. Ma, Prof. P. J. A. Kenis
International Institute for Carbon Neutral Energy Research (WPI-I²CNER)
Kyushu University
Fukuoka (Japan)

[d] Y. Lan
Key Laboratory of Green Chemistry and Chemical Process
Department of Chemistry, East China Normal University
3663N Zhongshan Road, Shanghai 200062 (China)

📃 Supporting Information for this article is available on the WWW under
http://dx.doi.org/10.1002/cssc.201300934.

high energy efficiency), high Faradaic efficiency (high selectivity), and high current density (thus high rate of conversion).[5,7]

Over the past decades multiple metal catalysts have been tested for the production of various products by the electrochemical reduction of CO_2.[6a,8] For example, Hori et al. found that different metal catalysts exhibit selectivity for different products, that is, metals such as Ag and Au lead to predominantly CO, metals such as Sn lead to formate, and Cu leads to the formation of mixtures of hydrocarbons.[9] Here, we focus on the conversion of CO_2 to CO as the combination of CO and H_2 (syngas) can be converted to liquid fuels through the Fischer–Tropsch process. Although some catalysts are able to produce CO and H_2 at the same time, we focus on catalysts that predominantly produce CO because H_2 can be obtained more efficiently (higher system efficiency and current density) from other sources, for example, water electrolysis, than by the cogeneration of H_2 with CO. Overall, the optimization of the electrolysis cell for CO production and the supply of H_2 from water electrolysis will be energetically more efficient than cogeneration in a single electrolyzer.[5]

Some early work indicates that the large overpotential needed for CO_2 reduction mainly stems from the barrier of the initial electron transfer to form a $CO_2^{.-}$ intermediate that is poorly stabilized by most metal surfaces.[4d,10] Some approaches to stabilize this intermediate to lead to a lower overpotential have been reported. Recently, we reported the use of 1-ethyl-3-methylimidazolium tetrafluoroborate (EMIM-BF$_4$) as a cocatalyst in combination with an unsupported Ag-nanoparticle-based catalyst to lower the cell overpotential for the electroreduction of CO_2 to CO on Ag to ~ 0.2 V, although only at low current densities (< 5 mA cm^{-2}) and high loading (6.67 mg of Ag per cm^2).[11] Chen et al. reduced the overpotential of CO_2 reduction to CO to 140 mV by stabilizing the $CO_2^{.-}$ intermediate on the surfaces of oxide-derived Au electrodes.[12] With respect to conversion, most studies that focus on the electroreduction of CO_2 to CO report current densities in the range of 2–118 mA cm^{-2} under ambient conditions, and most of these studies use Ag as the cathode catalyst.[7] For example, Dufek et al.[13] and Delacourt et al.[14] reported partial current densities for CO (j_{CO}) of less than 60 mA cm^{-2} at -1.8 V vs. Ag/AgCl if they operated their respective cells at ambient temperature and pressure. Tornow et al. studied N-based organometallic Ag catalysts, which achieved j_{CO} values as high as 115 mA cm^{-2} while the Ag loading was decreased by a factor of 20.[15] Recently, we have reported that the performance of Ag catalysts in CO_2 reduction depends on the Ag nanoparticle size.[16]

To date, significant efforts have focused on the exploration of catalysts, whereas significantly fewer studies have focused on the investigation of different catalyst supports. Catalyst supports can have tremendous influence on catalyst performance, which can result in lower catalyst loading.[17] For example, in fuel cells, the reduction of the loading of precious catalysts, especially Pt, while increasing performance and durability, has been a critical step towards the improvement of the commercial viability of this technology.[17] Specifically, support materials have been developed to support and stabilize smaller nanoparticles that are often more active to enable better catalyst

dispersion and utilization and provide better electron conduction and mass transport.[17,18]

TiO_2 has been used as a readily available support material and a catalyst for a variety of applications, which include as a noncarbonaceous support for Pt in fuel cell electrodes[19] and as a catalyst itself in the photoreduction of CO_2.[20] TiO_2 has been reported to interact strongly with Pt, which increases the Pt catalyst activity, stability, and durability.[17,21] TiO_2 can also act as a redox electron carrier to facilitate various reduction reactions, which include CO_2 conversion.[22] Additionally, the TiO_2 surface has been reported to assist in CO_2 adsorption,[23] thus it may be able to stabilize the $CO_2^{.-}$ intermediate to reduce the overpotential.

Here we report the use of TiO_2 as a catalyst support for Ag catalysts to improve the reduction of CO_2 to CO. Previously, Cueto et al. observed the enhancement of CO_2 and/or H_2O reduction with Ag particles (~ 250 nm) that are electrodeposited onto a thin-film TiO_2 electrode.[24] This work did not report product selectivity, and they did not study the role, if any, of the flat TiO_2 film. In contrast, the study reported here investigates the effect of much smaller, sub-10 nm Ag nanoparticles deposited on 15–30 nm TiO_2 particles on CO_2 electroreduction. Specifically, we synthesized and characterized two types of catalysts: different loadings of Ag catalyst supported on TiO_2 (Ag/TiO_2) and 40 wt % Ag supported on carbon black (Ag/C). We compared their electrochemical performance in the reduction of CO_2 to CO with the performance of the well-studied Ag nanoparticle catalysts by using an electrochemical flow reactor.[15,25] Through structural characterization and electrochemical experiments, we also investigated the role of the TiO_2 support in the enhancement of the catalytic sites, specifically with respect to its ability to maintain the Ag nanoparticles at their most catalytically active size and its ability to stabilize the $CO_2^{.-}$ intermediate.

Results and Discussion

Composition analysis

We synthesized catalysts composed of different amounts of Ag on a TiO_2 support and for comparison we also synthesized 40 wt % Ag on a carbon support (Vulcan XC-72R). Details of the synthesis of these catalysts are provided in the Experimental Section. The values for the actual Ag loading of the synthesized catalysts obtained by using inductively coupled plasma optical emission spectroscopy (ICP-OES) are summarized in Table 1. These values are in good agreement with the intended

Table 1. Ag composition of the synthesized catalysts.

Catalyst	Ag loading [wt %]	
	intended	actual
5 wt % Ag/TiO_2	5	1.67
10 wt % Ag/TiO_2	10	5.47
20 wt % Ag/TiO_2	20	18.94
40 wt % Ag/TiO_2	40	38.51
60 wt % Ag/TiO_2	60	54.20
40 wt % Ag/C	40	38.20

values except for the materials with low catalyst loadings, which can probably be explained by the relatively large loss of catalyst during the washing step as more frequent washing is required if a large amount of TiO_2 is added.

Catalyst performance in the flow reactor

Performance comparison of different support materials

The performance of the different Ag/TiO_2 and Ag/C catalysts was determined by using a flow reactor reported previously.[15,25] We used 1 M KOH as the electrolyte as it has a higher conductivity than other commonly used electrolytes for CO_2 reduction, such as K_2SO_4 and $KHCO_3$.[26] The geometric area of the electrode was used to calculate current densities. j_{CO} as a function of the cathode potential for four different cathode catalysts: 40 wt% Ag/TiO_2, 40 wt% Ag/C, AgNP, and plain TiO_2, which were immobilized on gas diffusion electrodes (GDE) by hand painting at an identical total cathode catalyst loading of 1 mg cm^{-2}, is shown in Figure 1 a. Ag/TiO_2 exhibits a better performance than Ag/C. Specifically, at −1.7 V vs. Ag/AgCl, j_{CO} for 40 wt% Ag/TiO_2 was 60 mA cm^{-2}, whereas 40 wt% Ag/C reached 28 mA cm^{-2}. So at this cathode potential, approximately twice the amount of CO is produced by using TiO_2 rather than carbon black as the support material for the Ag particles. Then, at a cathode potential of −1.8 V vs. Ag/AgCl, the j_{CO} observed for the 40 wt% Ag/TiO_2 catalysts was approximately 101 mA cm^{-2}, which is significantly higher than the value of approximately 62 mA cm^{-2} reported previously for a commercially available 'Silflon' Ag GDE at the same cathode potential.[26] If the performance observed with 40 wt% Ag/TiO_2 is compared to the value reported by Cueto et al. who used 250 nm Ag particles on flat TiO_2 films, we observed that 40 wt% Ag/TiO_2 exhibited a much higher performance in terms of current density (two orders of magnitude higher) and selectivity for products from CO_2 conversion, although the current density reported by Cueto et al. is the sum of CO_2 conversion and H_2O reduction.[24] Also, the current density achieved with 40 wt% Ag/TiO_2 is ~20 times higher than that achieved in our previous work,[11] but at a 15-times lower Ag loading: 0.4 vs. 6.67 mg of Ag per cm^2. The 40 wt% Ag/TiO_2 cathode and the AgNP cathode exhibit very similar performances (Figure 1 a). This result indicates that the Ag metal content can be drastically reduced without sacrificing performance if a Ag/TiO_2 catalyst is used, which improves its commercial viability for CO_2 reduction. The electrochemical surface area (ECSA) measurement of Ag described in the Supporting Information indicates that the ECSA of Ag in the 40 wt% Ag/TiO_2 electrode is much lower than the ECSA of Ag in the 40 wt% Ag/C or AgNP electrode, which underscores the important beneficial role of the TiO_2 support in the reduction of CO_2 and suggests the synergistic effect between Ag and TiO_2.

Interestingly, in the low current density regime, the 40 wt% Ag/TiO_2 cathode performed best (highest partial current density for CO), followed by the AgNP and 40 wt% Ag/C cathodes. This increased performance at low current density may be because of the increased adsorption of CO_2 and stabilization of
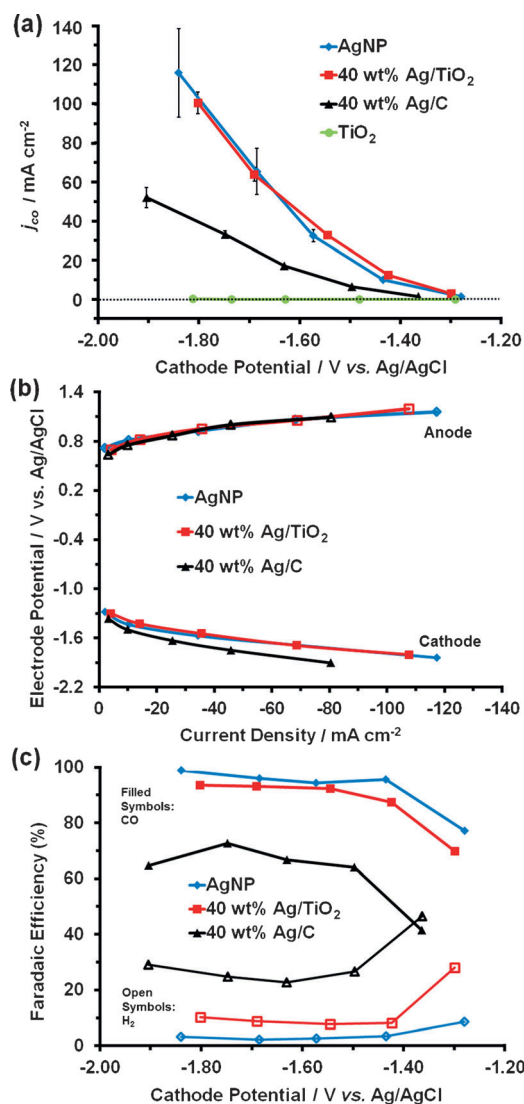

Figure 1. a) Partial current density for CO production with four catalysts: 40 wt% Ag/TiO_2, 40 wt% Ag/C, AgNP, and TiO_2; b) Single-electrode polarization curves and c) Faradaic efficiencies of 40 wt% Ag/TiO_2, 40 wt% Ag/C, and AgNP. The error bars represent the standard deviation of the average of three experiments ($N = 3$). Data collected at room temperature and ambient pressure; electrolyte: 1 M KOH; catalyst loading: 1 mg cm^{-2}; CO_2 stream: 7 sccm.

$CO_2$$^{−}$ by TiO_2. If plain TiO_2 was used as the cathode catalyst on a GDE (control experiment), no activity for CO production was observed, which confirms that the production of CO in the other experiments stems from the presence of Ag.

Single-electrode polarization curves for 40 wt% Ag/TiO_2, 40 wt% Ag/C, and AgNP are shown in Figure 1 b. The anode polarization curves are nearly identical because the same operating conditions, anode catalyst, and catalyst loading were used for all experiments. Therefore, the difference in total current densities can be attributed to differences in cathode performance. Naughton et al. developed a method to analyze polarization curves of individual fuel-cell electrodes by applying a linear fit in the Ohmic region to obtain a slope R_{Ohmic}.[27] A higher R_{Ohmic} value indicates a higher electrode resistance.[27]

R_{Ohmic} contains information about electrical resistances, any contact resistance between the electrolyte and electrode, and any mass transport losses. The R_{Ohmic} parameter is not based exclusively on electrical resistance but rather is the apparent resistance in the Ohmic region. By using this method, we found that the lower performance of the Ag/C catalyst relative to the Ag/TiO$_2$ and AgNP catalysts was because of a higher resistance as indicated by a larger R_{Ohmic} despite the fact that carbon black has a higher conductivity, which implies that in this case R_{Ohmic} mainly originates from the contact resistance between the electrolyte and electrode as well as mass transport in both electrolyte and gas reactants rather than from the resistance caused by the low conductivity of support materials. Specifically, the carbon black support material is more hydrophobic and porous compared to the TiO$_2$ support material (Figure S2), which hampers contact between the Ag particles and the electrolyte. Also, compared to Ag/C, a thinner catalyst layer could be obtained for the Ag/TiO$_2$ catalyst at the same Ag loading because TiO$_2$ has a twofold higher density than carbon, which has improved mass transfer kinetics as previously reported.[19]

The Faradaic efficiencies (see SI for details on the calculation) for CO, the desired product, and H$_2$, the byproduct, as obtained for GDEs covered with 40 wt% Ag/TiO$_2$, 40 wt% Ag/C, and AgNP catalysts, respectively, are shown in Figure 1c. Among these three catalysts, AgNP achieved the highest Faradaic efficiency for CO > 95%. Ag/TiO$_2$ achieved a Faradaic efficiency for CO of 93%, whereas Ag/C achieved only 70% and much larger amounts of the byproduct H$_2$ were formed. Therefore, the low performance (i.e., the low partial current density) exhibited by Ag/C can be explained by its low Faradaic efficiency for CO, in addition to a higher electrode resistance (vide supra).

The effect of Ag loading on the Ag/TiO$_2$ performance

We also studied the performance of Ag/TiO$_2$ catalysts as a function of increasing Ag loading (5, 10, 20, 40, and 60 wt% Ag/TiO$_2$). Plots of the partial current density and Faradaic efficiency for CO versus the cathode potential for GDEs prepared with these catalysts with a constant total catalyst loading of 1 mg cm^{-2} are shown in Figure 2a and b. In general (for the 5–40 wt% samples), the data indicated that the higher the Ag loading, the higher the partial current density and Faradaic efficiency for CO, especially at more negative cathode potentials (from −1.5 to −1.8 V vs. Ag/AgCl). TEM micrographs of the Ag/TiO$_2$ catalysts with different Ag loadings suggest that this trend can be explained by the increased number of Ag particles exposed on the TiO$_2$ surface (Figure 3). Interestingly, the 60 wt% Ag/TiO$_2$ catalyst did not follow this trend. Its partial current density and Faradaic efficiency for CO were much lower than those observed for the 40 wt% Ag/TiO$_2$ especially at negative cathode potentials. TEM images of the 60 wt% samples suggest that Ag particles are more prone to agglomerate than the 40 wt% sample during reaction (compare Figure 3e and e', and histograms in Figure S4f and S4g) as the Ag particles are more densely arranged on the support in sam-
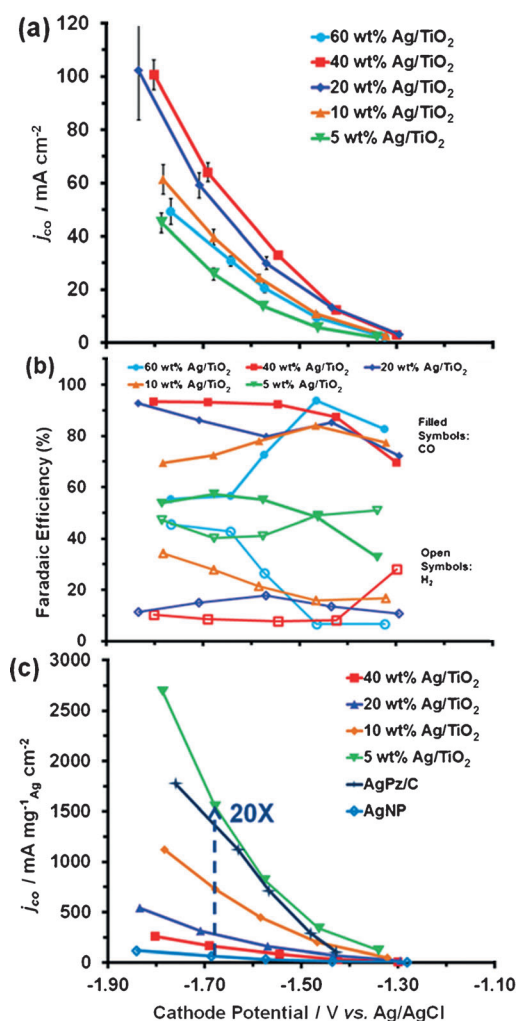

Figure 2. a) Partial current density for CO and b) Faradaic efficiency of Ag/TiO$_2$ catalysts with different Ag loadings: 5, 10, 20, 40, and 60 wt%; c) Partial current densities for CO vs. cathode potential relative to the cathode Ag loading for different catalysts. The error bars represent the standard deviation of the average of three experiments ($N = 3$). Data collected at room temperature and ambient pressure; electrolyte: 1 M KOH; catalyst loading: 1 mg cm^{-2}; CO$_2$ stream: 7 sccm.

ples with a high loading, which increases the possibility for aggregation (compare Figure 3e and e'). The other possible reason for the lower performance of the 60 wt% sample is that according to the synergistic effect between Ag and TiO$_2$ (introduced later), an optimum Ag content, 40 wt% in this work, exists among the different Ag/TiO$_2$ catalysts. Catalysts with a Ag content higher or lower than 40 wt% exhibit a lower performance. Similar trends and explanations have been reported for other supported catalysts, for example, for Ag supported on carbon black in fuel-cell applications.[28]

One of the main advantages of the Ag/TiO$_2$ catalysts studied in this paper is their low mass fraction of Ag, which reduces the amount of precious metal needed. The performance per mass Ag (i.e., the mass activity) for all catalysts used in this study is compared in Figure 2c. For example, the mass activity of 5 wt% Ag/TiO$_2$ was 20-fold higher than that of the commercial AgNP catalyst and much higher than the mass activity of
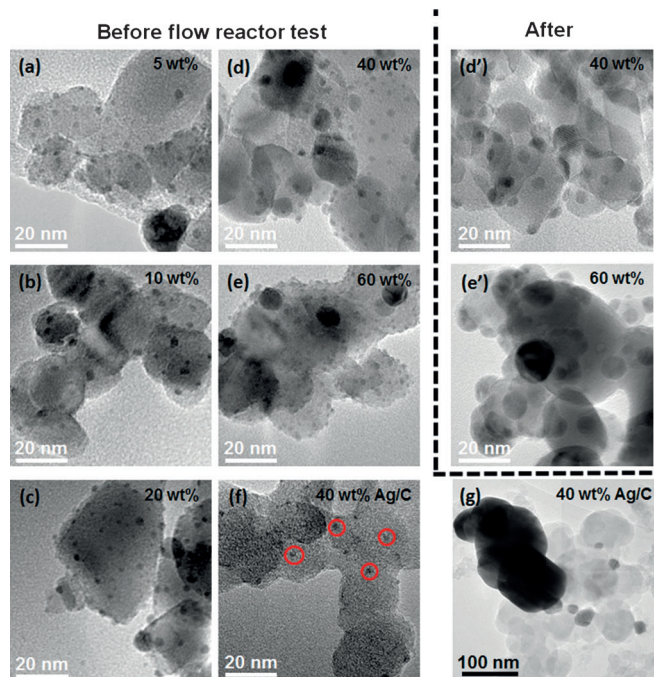
Figure 3. TEM images of the synthesized catalysts before the flow-reactor test: a) 5 wt% Ag/TiO$_2$; b) 10 wt% Ag/TiO$_2$; c) 20 wt% Ag/TiO$_2$; d) 40 wt% Ag/TiO$_2$; e) 60 wt% Ag/TiO$_2$; f) 40 wt% Ag/C with higher magnification; g) 40 wt% Ag/C with lower magnification; and after the flow-reactor test: d') 40 wt% Ag/TiO$_2$; e') 60 wt% Ag/TiO$_2$. Dark spheres or dots are Ag particles; the grey larger structures are the support materials. The dots in red circles are examples of Ag particles in the pores or recesses of the carbon support.

N-based Ag catalysts (e.g., Ag pyrazole, AgPz), which we reported previously with a high mass activity of 1600 mA m-g$_{Ag}^{-1}$ cm^{-2} at −1.7 V vs. Ag/AgCl.[10] In addition, all of the Ag/TiO$_2$ catalysts showed relatively high cell energy efficiencies (see SI for details on the calculation). For example, the cell energy efficiency was 65% at a cell potential of −2 V for the 40 wt% Ag/TiO$_2$ catalyst, compared to only 50% for the 40 wt% Ag/C catalyst and 56% for the AgNP catalyst.

Ag particle size and size distribution

To explain the high performance of the GDEs covered with Ag/TiO$_2$ catalysts in the flow reactor, we characterized the catalysts with respect to size and the size distribution of the nanoparticles supported by TiO$_2$ or carbon black both before and after flow-reactor tests (Figure 3). The histograms of the Ag particle size distribution are shown in Figure S4. The synthetic method used here (see Experimental Section) yields more uniform and much smaller Ag particles that are at their active size (< 10 nm) and dispersed well on the TiO$_2$ (Figure 3 a–e), especially if compared to the > 200 nm electrodeposited Ag particles reported previously.[24] However, for the Ag/C sample, both small (< 10 nm) and large Ag particles (> 100 nm) can be found on the carbon black (Figure 3 f and g). Some of the Ag particles tend to agglomerate to yield larger Ag particles for metal loadings higher than 40 wt% (Figure 3 d and e).

Importantly, as shown in Figure 3 a–3 e, most of the Ag particles in the Ag/TiO$_2$ catalysts are supported on the surface of TiO$_2$, whereas in the Ag/C sample, for those sections with small Ag particles, much fewer Ag particles are exposed on the surface; instead the Ag particles are trapped in deep micropores or recesses (black dots highlighted by red circles in Figure 3 f), presumably because of the porous nature of the carbon support. Although images from TEM tomography would be more straightforward, the above result is in agreement with previous work.[17] The less exposed nature of the Ag particles in the Ag/C sample makes them less accessible for CO$_2$ and the electrolyte, which, in addition to the presence of agglomerated large Ag particles in the sample, may explain the higher selectivity for CO formation over H$_2$ evolution (a higher Faradaic efficiency for CO) exhibited by, for example, the 40 wt% Ag/TiO$_2$ catalyst than by the 40 wt% Ag/C catalyst. Although the competing H$_2$ evolution reaction can be catalyzed by both exposed carbon and TiO$_2$, Ag/C exposes a larger surface area of the carbon support to the electrolyte (compared to the surface area of the TiO$_2$ support exposed in Ag/TiO$_2$), which, therefore, produces two to three times more H$_2$ than Ag/TiO$_2$ (Figure 1).

In summary, structural characterization by using TEM indicates that the surface of TiO$_2$ is able to accommodate small and well dispersed Ag particles that are not prone to sintering during experiments for the electrocatalytic conversion of CO$_2$ to CO. This is in accordance with prior observations for different catalysts and different reactions that TiO$_2$ is able to improve the anchorage of the catalyst nanoparticles on its surface while at the same time reducing agglomeration.[19, 21a, 29]

Catalyst activity in a standard three-electrode cell

The performance towards CO$_2$ reduction for the Ag/TiO$_2$ catalyst compared to the AgNP and Ag/C catalysts was also studied by using cyclic voltammetry (CV) in a standard three-electrode cell. K$_2$SO$_4$ (0.5 M), a widely used electrolyte in CO$_2$ reduction studies,[13] was used here. In a standard three-electrode cell, KOH would react with CO$_2$ to form carbonate/bicarbonate, which would, therefore, decrease the electrolyte pH significantly (from 13.58 to 9.96) and thus the amount of the active species, molecular CO$_2$. However, we can use a KOH solution as the electrolyte in the flow reactor because once CO$_2$ diffuses through the GDE, it reacts at the triple boundary phase[18b] to form CO, and the reaction of CO$_2$ with KOH could be minimized.[26] In fact, the flowing electrolyte will refresh the surface and minimize the pH decrease (from 13.65 to 13.48). Therefore, KOH can be used as an electrolyte to increase the electrolyte conductivity in the flow cell, and K$_2$SO$_4$ is a better option than KOH in the three-electrode cell. Either CO$_2$ or Ar gas was bubbled through the electrolyte for 15 min prior to CV measurements. As shown in Figure 4 a, b, and c, extensive H$_2$ evolution is observed on both the Ag and Ag/TiO$_2$ electrodes in the Ar-saturated electrolyte. However, if we used a CO$_2$-saturated electrolyte, different reduction peaks with different onset potentials and lower peak currents, presumably associated with CO$_2$ reduction, were observed for both catalysts. The smaller reduction peak current observed if a CO$_2$-saturated electrolyte
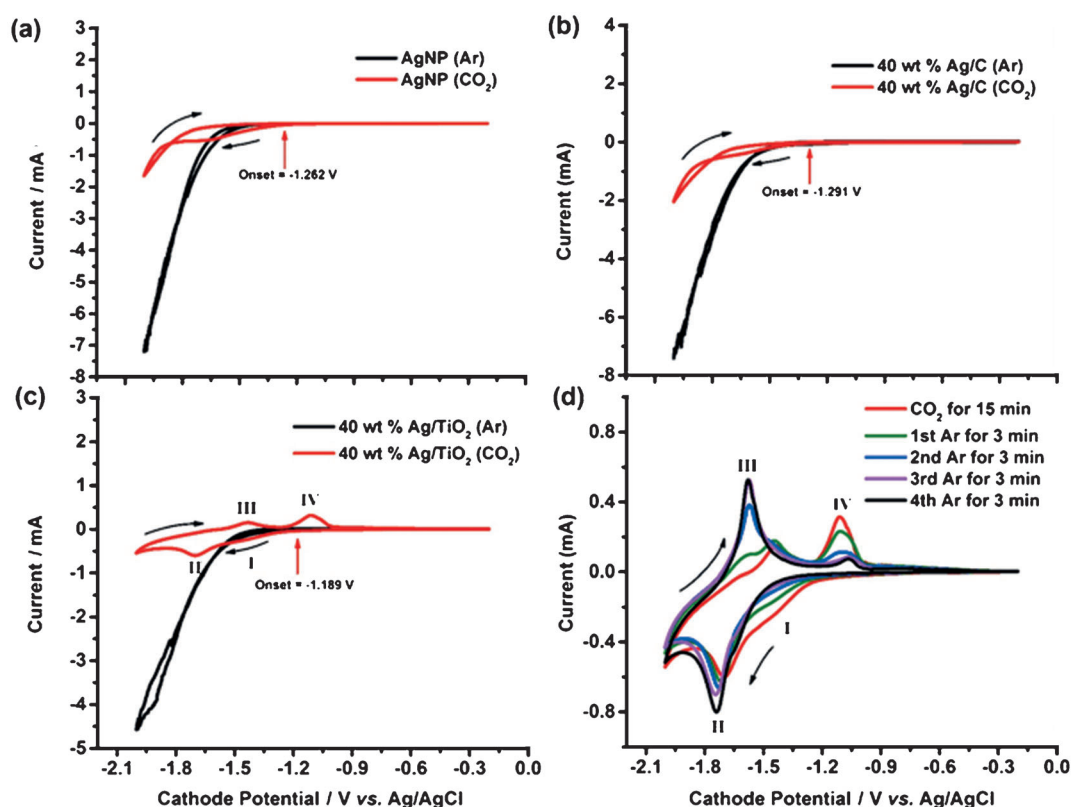
Figure 4. CV of a) AgNP, b) 40 wt% Ag/C, and c) 40 wt% Ag/TiO$_2$ catalysts after bubbling Ar (black) or CO$_2$ (red). The instability in the black curves is probably because of the evolution of large amounts of H$_2$. d) CV of 40 wt% Ag/TiO$_2$ catalyst after bubbling CO$_2$ (red) or Ar (other colors). All experiments used K$_2$SO$_4$ (0.5 M) as the electrolyte and 25 mV s^{-1} as the scan rate.

was used is probably because of the inhibition of the H$_2$ evolution reaction by the species that are adsorbed during CO$_2$ reduction.[6a] The Ag/TiO$_2$ catalyst (Figure 4c) exhibits a 73 mV lower onset potential for CO$_2$$^{·-}$ formation (and thus a lower overpotential) than the AgNP catalyst (Figure 4a): -1.189 and -1.262 V vs. Ag/AgCl at $i = -0.04$ mA, and 102 mV lower onset potential for CO$_2$$^{·-}$ formation than the Ag/C catalyst, respectively. The large overpotential typically observed for CO$_2$ reduction has been attributed to the barrier of the initial electron transfer to form a CO$_2$$^{·-}$ intermediate, which is poorly stabilized by most metal surfaces.[4d, 11] Thus, the improvement observed here may be because of the adsorption and stabilization of CO$_2$$^{·-}$ on the TiO$_2$ surface. This may be further proved by the CV study shown in Figure S6a, in which TiO$_2$ alone as a catalyst also exhibits a low onset potential of -1.196 V vs. Ag/AgCl for the conversion of CO$_2$ to CO$_2$$^{·-}$$_{ads}$. This observation of an earlier onset potential for Ag/TiO$_2$ is also in agreement with the better performance of the Ag/TiO$_2$ catalyst compared to the AgNP catalyst in the lower current density regime and compared to the Ag/C catalyst in the whole current density range in the flow-reactor test (Figure 1a). Therefore, both the experiments in the flow reactor and in the standard three-electrode cell with different electrolytes show that Ag/TiO$_2$ performs better than Ag/C and even pure AgNP.

Interestingly, another reduction peak at around -1.7 V vs. Ag/AgCl and two anodic peaks were also observed for the Ag/TiO$_2$ catalyst compared to the AgNP catalyst. To explain those

peaks, Ar was bubbled into the solution for 3 min to remove some CO$_2$ after the CV scan was recorded in the CO$_2$-saturated electrolyte (Figure 4c). The bubbling of Ar was repeated four times, and CV measurements were recorded each time after Ar was bubbled into the solution. As shown in Figure 4d, if a relatively large amount of CO$_2$ was present in the electrolyte, two reductive (I and II) and oxidative peaks (III and IV) were observed. As the amount of CO$_2$ decreased, the intensities of peaks I and IV decreased, whereas that of peak III started to increase. The decrease in peak intensity indicates that peak I is related to the direct electrochemical reduction of CO$_{2 ads}$ to CO$_2$$^{·-}$$_{ads}$. The similar trend observed for peak IV is probably because of the oxidation of CO$_2$$^{·-}$$_{ads}$. The other two peaks, II and III, can thus be attributed to the reactions for TiO$_2$ and Ti^{III} species, which can indeed act as a redox electron carrier to facilitate some reactions, which include CO$_2$ reduction.[22b, c] There have been reports that the interfacial pH can be quite different from the bulk pH in unbuffered solutions, which affects the reaction rate.[30] In this case, we did not use a buffered solution because we did not want the adsorption/desorption peaks from the anions in the buffer solution to interfere with any observed redox species. A similar experiment that used TiO$_2$ without Ag (Figure S6a) confirms the redox behavior of Ti^{IV}/Ti^{III} for CO$_{2 ads}$ reduction to CO$_2$$^{·-}$$_{ads}$. Direct reduction of CO$_2$ by using TiO$_2$ as the catalyst is possible, however, a negligible amount of CO was observed if only TiO$_2$ was used, whereas Ag/TiO$_2$ is able to produce a much larger amount of CO in K$_2$SO$_4$ (0.5 M)
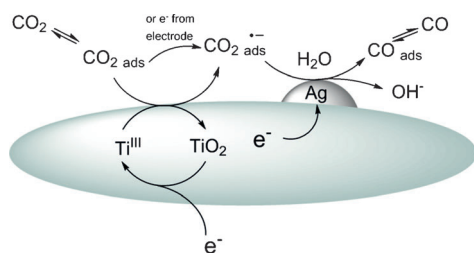
Figure 5. A schematic diagram of the proposed pathway for CO_2 reduction to CO on the Ag/TiO$_2$ catalyst.

electrolyte in the flow reactor (Figure S6b), which indicates that the production of CO requires the presence of Ag on TiO$_2$.

A schematic that describes the proposed reaction pathway of the reduction of CO_2 on a Ag/TiO$_2$ catalyst is shown in Figure 5. CO_2 is first adsorbed on TiO$_2$. At less negative cathode potentials (more positive than the redox potential of the Ti^{IV}/Ti^{III} couple), the adsorbed CO_2 gains one electron from the electrode and is converted to $CO_2^{\cdot-}$. Then the produced $CO_2^{\cdot-}$ is adsorbed and stabilized on the TiO$_2$ surface, which results in a decrease of the overpotential for this step. At more negative cathode potentials, the Ti^{III} species (which has been reported to form upon thermal annealing in a vacuum,[23c] is known to facilitate CO_2 adsorption, and can act as the active sites for CO_2 photoreduction[31]) is formed by the reduction of TiO$_2$. Then, the adsorbed CO_2 species is reduced either by one electron from the electrode or by the produced Ti^{III} species to form $CO_2^{\cdot-}$ads. The Ti^{III} is then oxidized back to TiO$_2$. This cycle is in agreement with the observed decrease in the intensity of the anodic peak III in the presence of a relatively large amount of CO_2 in the solution as most of the Ti^{III} species are used to reduce CO_2 rather than oxidized by the electrode on the reverse sweep (peak III). The involvement of these oxygen-vacancy Ti^{III} species may improve the stabilization of $CO_2^{\cdot-}$ads, which thereby facilitates this process and increases the activity of this catalyst to be comparable to AgNP at even lower Ag loadings. Once formed, $CO_2^{\cdot-}$ads is further reduced to CO$_{ads}$ under the catalytic influence of Ag in the presence of H_2O. The combination of the observation that the Ag/TiO$_2$ catalyst was able to produce CO at a lower onset potential than the Ag catalyst and the observation that TiO$_2$ alone is not able to produce CO strongly suggests that the observed enhancement in the performance can be attributed to a synergistic effect between Ag and TiO$_2$.

Conclusions

We showed that Ag supported on TiO$_2$ outperforms Ag supported on carbon black in the reduction of CO_2 to CO, whereas Ag/TiO$_2$ performs at a similar absolute level as unsupported Ag nanoparticles, for which the Faradaic efficiency for CO exceeds 90% and the current density exceeds 100 mA cm^{-2}. Compared to carbon black, TiO$_2$ is a superior support for Ag catalysts for the electrochemical reduction of CO_2 to CO, because (1) TiO$_2$ helps to create small, well-dispersed Ag particles at their active size (sub-10 nm) on the TiO$_2$ surface; (2) TiO$_2$ improves the sta-

bility of these Ag particles (minimizes agglomeration during the synthesis); (3) TiO$_2$ improves CO_2 reduction kinetics, probably through the adsorption and stabilization of the $CO_2^{\cdot-}$ intermediate, which then can react to form CO on adjacent Ag particles. In contrast, Ag particles supported by carbon black are not as well dispersed, not as stable during the synthesis, and do not appear to enhance the reaction kinetics.

By using TiO$_2$ as the support, the Ag loading can be reduced without sacrificing performance towards selective CO production. 40 wt% Ag/TiO$_2$ is able to produce the same amount of CO as unsupported AgNP, but at a 2.5 times lower Ag loading. Furthermore, the 5 wt% Ag/TiO$_2$ catalyst achieved a mass activity as high as 2700 mA mg$_{Ag}^{-1}$ cm^{-2}. Ag is 5–10 times more expensive than TiO$_2$, therefore, supporting Ag particles on TiO$_2$ enhances the promise of these catalyst for the development of an economically viable process for the electrochemical reduction of CO_2 to CO.

We also studied the role of TiO$_2$ as a support material during the electrochemical reduction of CO_2. Based on cyclic voltammetry data, a reaction pathway is proposed that involves the participation of Ti^{IV}/Ti^{III} from the support material, which acts as the redox couple and stabilizes the reaction intermediate. Further research is needed to confirm the proposed reaction pathway. For example, calculations and spectroscopic experiments could guide these efforts with respect to the prediction and confirmation of the adsorption/stabilization of intermediates and the interactions between metal particles and support materials.

Further studies could also focus on the exploration of other metal catalysts supported by metal oxide semiconductors such as CeO$_2$. Such catalysts may be able to modify the adsorption isotherms for the intermediates and be able to further decrease the energy barrier for the electrochemical reduction of CO_2.

Experimental Section

Preparation of Ag/TiO$_2$ and Ag/C catalysts

The previously reported citrate-protecting method[28, 32] was used to obtain the different Ag/TiO$_2$ catalysts. In contrast to previous reports, the support materials used here (TiO$_2$ or carbon black) were first mixed with AgNO$_3$ (40 mM; Sigma–Aldrich) aqueous solution to allow the better adsorption of Ag$^+$ on the support. Sodium citrate (Fisher Chemicals) was then added to stabilize Ag$^+$ followed by the addition of NaBH$_4$ (Sigma–Aldrich) to reduce Ag$^+$. Specifically, for the synthesis of 40 wt% Ag/TiO$_2$, AgNO$_3$ (125.7 mg) was dissolved in Millipore H_2O (18.5 mL). TiO$_2$ (120 mg, Aeroxide TiO$_2$ P25, particle size: 21±5 nm) was added to the solution, and the mixture was stirred for 30 min. Subsequently, sodium citrate solution (131 mM, 18.5 mL) was added dropwise with stirring. The reduction of Ag$^+$ was achieved by the dropwise addition of NaBH$_4$ solution (30 mM, 25 mL) with vigorous stirring in an ice bath. After stirring the solution gently overnight, it was centrifuged, washed, and dried in a vacuum oven at 80 °C for 4 h. The obtained catalyst was wine red in color. Samples with Ag loadings of 5, 10, 20, and 60 wt% were prepared by using the same method by changing the amount of TiO$_2$. For comparison, 40 wt% Ag/C catalyst was

synthesized with the same method by using Vulcan XC-72R (Carbon Blk Vulcan XC-72R, Fuel Cell Store) as the support.

Physical characterization

The Ag weight percentages of the different catalysts were determined by using ICP-OES (PerkinElmer-Optima 2000DV). The samples were digested in a mixture of HNO_3 and HF prior to analysis. The Ag particle size and dispersion on the support were examined by using TEM (JOEL 2100 CRYO) operated at 200 kV. The TEM sample was prepared by suspending the catalyst in isopropanol and placing a drop of the suspension onto a holey carbon-coated 200 mesh grid followed by solvent evaporation overnight at RT.

Electrochemical characterization

Electrode preparation: Catalyst inks were prepared by mixing Millipore water (200 μL), catalyst (2 mg), Nafion solution (2.6 μL, 5 wt%, Fuel Cell Earth), and isopropyl alcohol (200 μL). The inks were then sonicated (Vibra-Cell ultrasonic processor, Sonics & Materials) for 15 min and then painted on the microporous layer of Sigracet 35 BC gas diffusion layers (Ion Power) with a paintbrush. All of the flow-reactor experiments in this study used a 1 mg cm^{-2} cathode catalyst loading on Sigracet 35BC, and all of the anodes used in this study had a 1 mg cm^{-2} Pt loading on Sigracet 35BC.

Electrochemical flow reactor operation: The flow reactor (see SI for a schematic) was operated under ambient conditions. A potentiostat (Autolab PGSTAT-30, EcoChemie) operating in steady-state chronoamperometric mode was used to measure the resulting current as reported previously.[15] For each trial, five cell potentials from −2.0 to −3.0 V with an interval of 0.25 V was applied to the cell. For each potential, the cell was allowed to reach steady state for 200 s, after which the gas flowed into a gas chromatograph. The current was averaged for an additional 180 s before stepping to the next potential. The individual electrode potentials were measured by using multimeters (AMPROBE 15XP-B) connected to each electrode and a Ag/AgCl reference electrode (RE-5B, BASi) placed in the exit stream. A mass flow controller (MASS-FLO, MKS instrument) was used to flow CO_2 from a cylinder at 7 sccm. A syringe pump (PHD 2000, Harvard Apparatus) supplied the 1 M KOH electrolyte at 0.5 mL min^{-1}. Gas products that formed on the GDE surface left through the GDE to the gas stream driven by a vacuum connected to the end of the gas channel. For the composition analysis of H_2 and CO, the effluent gas stream flowed directly into a gas chromatograph (Thermo Finnegan Trace GC) operating in the thermal conductivity detection (TCD) mode, with a Carboxen 1000 column (Supelco) and He as the carrier gas at a flow rate of 20 sccm. The column was held at 150 °C, and the TCD detector was held at 200 °C. The only cathode products detected by GC were CO and H_2 if Ag was used as the catalyst, consistent with results reported previously.[26,33] Other products that could not be detected by GC may have formed as well but only in very small amounts (< 4% for 40 wt% Ag/TiO_2 and AgNP; < 10% for 40 wt% Ag/C). The analysis of these minor products was beyond the scope of this study. After each trial to test 40 wt% Ag/TiO_2 and 60 wt% Ag/TiO_2, the catalysts were further characterized by TEM.

Three-electrode cell operation: CVs were measured by using a standard three-electrode cell, which consisted of a Pt gauze (100 mesh, 99.9% metals basis, Sigma–Aldrich, 25 × 25 mm^2) counter electrode and a Ag/AgCl reference electrode (RE-5B, BASi) separated from the working electrode by a Luggin capillary. The three-electrode cell experiments were performed by using a potentiostat (Autolab PGSTAT302N, EcoChemie). Catalyst inks were prepared according to the method described above. The catalyst layer for the three-electrode cell experiments was prepared as follows: a drop of the catalyst ink (5 μL) was deposited (and then dried under flowing Ar) on a rotating disk electrode (Metrohm 6.1204.300), which had a polished (0.05 micron alumina) glassy carbon disk electrode surface ($d = 3$ mm, $S = 0.07065$ cm^2). All CV measurements in this study were conducted in K_2SO_4 (0.5 M) at a scan rate of 25 mV s^{-1}.

[1] a) A. T. Bell, *Basic Research Needs, Catalysis for Energy* 2008, U.S. Department of Energy, Bethesda, MD; b) P. Taylor, *Energy Technology Perspectives* 2010, International Energy Agency.

[2] S. Pacala, R. Socolow, *Science* 2004, 305, 968–972.

[3] a) N. S. Lewis, *Science* 2007, 315, 798–801; b) J. C. Meier, I. Katsounaros, C. Galeano, H. J. Bongard, A. A. Topalov, A. Kostka, A. Karschin, F. Schuth, K. J. J. Mayrhofer, *Energy Environ. Sci.* 2012, 5, 9319–9330.

[4] a) M. Gattrell, N. Gupta, A. Co, *J. Electroanal. Chem.* 2006, 594, 1–19; b) P. Galindo Cifre, O. Badr, *Energy Convers. Manage.* 2007, 48, 519–527; c) C. Oloman, H. Li, *ChemSusChem* 2008, 1, 385–391; d) Y. Hori in *Handbook of Fuel Cells, Vol. 2*, Wiley, 2010, pp. 720–733; e) M. Mikkelsen, M. Jorgensen, F. C. Krebs, *Energy Environ. Sci.* 2010, 3, 43–81; f) S. Bensaid, G. Centi, E. Garrone, S. Perathoner, G. Saracco, *ChemSusChem* 2012, 5, 500–521; g) B. Kumar, M. Llorente, J. Froehlich, T. Dang, A. Sathrum, C. P. Kubiak, *Annu. Rev. Phys. Chem.* 2012, 63, 541–569; h) S. Dahl, I. Chorkendorff, *Nat. Mater.* 2012, 11, 100–101.

[5] D. T. Whipple, P. J. A. Kenis, *J. Phys. Chem. Lett.* 2010, 1, 3451–3458.

[6] a) Y. Hori in *Modern Aspects of Electrochemistry, Vol. 42* (Eds.: C. Vayenas, R. White, M. Gamboa-Aldeco), Springer, New York, 2008, pp. 89–189; b) G. Centi, E. A. Quadrelli, S. Perathoner, *Energy Environ. Sci.* 2013, 6, 1711–1731.

[7] H.-R. M. Jhong, S. Ma, P. J. A. Kenis, *Curr. Opin. Chem. Eng.* 2013, 2, 191–199.

[8] a) Y. Hori, K. Kikuchi, S. Suzuki, *Chem. Lett.* 1985, 1695–1698; b) S. Ikeda, T. Takagi, K. Ito, *Bull. Chem. Soc. Jpn.* 1987, 60, 2517–2522; c) M. Azuma, K. Hashimoto, M. Hiramoto, M. Watanabe, T. Sakata, *J. Electrochem. Soc.* 1990, 137, 1772–1778; d) A. S. Agarwal, Y. M. Zhai, D. Hill, N. Sridhar, *ChemSusChem* 2011, 4, 1301–1310; e) K. P. Kuhl, E. R. Cave, D. N. Abram, T. F. Jaramillo, *Energy Environ. Sci.* 2012, 5, 7050–7059.

[9] Y. Hori, H. Wakebe, T. Tsukamoto, O. Koga, *Electrochim. Acta* 1994, 39, 1833–1839.

[10] K. Chandrasekaran, L. O. M. Bockris, *Surf. Sci.* 1987, 185, 495–514.

[11] B. A. Rosen, A. Salehi-Khojin, M. R. Thorson, W. Zhu, D. T. Whipple, P. J. A. Kenis, R. I. Masel, *Science* 2011, 334, 643–644.

[12] Y. Chen, C. W. Li, M. W. Kanan, *J. Am. Chem. Soc.* 2012, 134, 19969–19972.

[13] E. Dufek, T. Lister, M. McIlwain, *J. Appl. Electrochem.* 2011, 41, 623–631.

[14] C. Delacourt, P. L. Ridgway, J. B. Kerr, J. Newman, *J. Electrochem. Soc.* 2008, 155, B42–B49.

[15] C. E. Tornow, M. R. Thorson, S. Ma, A. A. Gewirth, P. J. A. Kenis, *J. Am. Chem. Soc.* 2012, 134, 19520–19523.

[16] A. Salehi-Khojin, H.-R. M. Jhong, B. A. Rosen, W. Zhu, S. Ma, P. J. A. Kenis, R. I. Masel, *J. Phys. Chem. C* 2013, 117, 1627–1632.

[17] S. Sharma, B. G. Pollet, *J. Power Sources* **2012**, *208*, 96–119.

[18] a) X. Wang, I. M. Hsing, P. L. Yue, *J. Power Sources* **2001**, *96*, 282–287; b) R. O'Hayre, D. M. Barnett, F. B. Prinz, *J. Electrochem. Soc.* **2005**, *152*, A439–A444; c) J. H. Bang, K. Han, S. E. Skrabalak, H. Kim, K. S. Suslick, *J. Phys. Chem. C* **2007**, *111*, 10959–10964.

[19] S.-Y. Huang, P. Ganesan, S. Park, B. N. Popov, *J. Am. Chem. Soc.* **2009**, *131*, 13898–13899.

[20] a) T. Inoue, A. Fujishima, S. Konishi, K. Honda, *Nature* **1979**, *277*, 637–638; b) K. Kočí, K. Matějů, L. Obalová, S. Krejčíková, Z. Lacný, D. Plachá, L. Čapek, A. Hospodková, O. Šolcová, *Appl. Catal. B* **2010**, *96*, 239–244; c) Y. Li, W.-N. Wang, Z. Zhan, M.-H. Woo, C.-Y. Wu, P. Biswas, *Appl. Catal. B* **2010**, *100*, 386–392; d) X. Li, Z. Zhuang, W. Li, H. Pan, *Appl. Catal. A* **2012**, *429–430*, 31–38.

[21] a) S. Y. Huang, P. Ganesan, B. N. Popov, *Appl. Catal. B* **2011**, *102*, 71–77; b) S. J. Tauster in *Strong Metal–Support Interactions, Vol. 298*, American Chemical Society, **1986**, pp. 1–9.

[22] a) F. Beck, W. Gabriel, *Angew. Chem.* **1985**, *97*, 765–767; *Angew. Chem. Int. Ed. Engl.* **1985**, *24*, 771–772; b) C. Ravichandran, C. J. Kennady, S. Chellammal, S. Thangavelu, P. N. Anantharaman, *J. Appl. Electrochem.* **1991**, *21*, 60–63; c) D. Chu, G. Qin, X. Yuan, M. Xu, P. Zheng, J. Lu, *ChemSusChem* **2008**, *1*, 205–209.

[23] a) K. Tanaka, K. Miyahara, I. Toyoshima, *J. Phys. Chem.* **1984**, *88*, 3504–3508; b) A. Markovits, A. Fahmi, C. Minot, *THEOCHEM* **1996**, *371*, 219–235; c) T. L. Thompson, O. Diwald, J. T. Yates, *J. Phys. Chem. B* **2003**, *107*, 11700–11704; d) L. F. Cueto, G. A. Hirata, E. M. Sanchez, *J. Sol-Gel Sci. Technol.* **2006**, *37*, 105–109.

[24] L. F. Cueto, G. T. Martinez, G. Zavala, E. M. Sanchez, *J. Nano Res.* **2010**, *9*, 89–100.

[25] D. T. Whipple, E. C. Finke, P. J. A. Kenis, *Electrochem. Solid-State Lett.* **2010**, *13*, B109–B111.

[26] E. J. Dufek, T. E. Lister, M. E. McIlwain, *Electrochem. Solid-State Lett.* **2012**, *15*, B48–B50.

[27] M. S. Naughton, A. A. Moradia, P. J. A. Kenis, *J. Electrochem. Soc.* **2012**, *159*, B761–B769.

[28] S. Maheswari, P. Sridhar, S. Pitchumani, *Electrocatalysis* **2012**, *3*, 13–21.

[29] C.-C. Shih, J.-R. Chang, *J. Catal.* **2006**, *240*, 137–150.

[30] a) I. Katsounaros, J. C. Meier, S. O. Klemm, A. A. Topalov, P. U. Biedermann, M. Auinger, K. J. J. Mayrhofer, *Electrochem. Commun.* **2011**, *13*, 634–637; b) M. Auinger, I. Katsounaros, J. C. Meier, S. O. Klemm, P. U. Biedermann, A. A. Topalov, M. Rohwerder, K. J. J. Mayrhofer, *Phys. Chem. Chem. Phys.* **2011**, *13*, 16384–16394.

[31] V. P. Indrakanti, H. H. Schobert, J. D. Kubicki, *Energy Fuels* **2009**, *23*, 5247–5256.

[32] J. Guo, A. Hsu, D. Chu, R. Chen, *J. Phys. Chem. C* **2010**, *114*, 4324–4330.

[33] E. J. Dufek, T. E. Lister, S. G. Stone, M. E. McIlwain, *J. Electrochem. Soc.* **2012**, *159*, F514–F517.